EDGE ARTICLE

Expanding excitation wavelengths for azobenzene photoswitching into the near-infrared range *via* endothermic triplet energy transfer†

Jussi Isokuortti,[a] Kim Kuntze,[a] Matti Virkki,[a] Zafar Ahmed, [iD][a] Elina Vuorimaa-Laukkanen,[a] Mikhail A. Filatov,[b] Andrey Turshatov, [iD][c] Timo Laaksonen,[ad] Arri Priimagi [iD] *[a] and Nikita A. Durandin*[a]

Developing azobenzene photoswitches capable of selective and efficient photoisomerization by long-wavelength excitation is an enduring challenge. Herein, rapid isomerization from the *Z*- to *E*-state of two *ortho*-functionalized bistable azobenzenes with near-unity photoconversion efficiency was driven by triplet energy transfer upon red and near-infrared (up to 770 nm) excitation of porphyrin photosensitizers in catalytic micromolar concentrations. We show that the process of triplet-sensitized isomerization is efficient even when the sensitizer triplet energy is substantially lower (>200 meV) than that of the azobenzene used. This makes the approach applicable for a wide variety of sensitizer-azobenzene combinations and enables the expansion of excitation wavelengths into the near-infrared spectral range. Therefore, indirect excitation *via* endothermic triplet energy transfer provides efficient and precise means for photoswitching upon 770 nm near-infared light illumination with no chemical modification of the azobenzene chromophore, a desirable feature in photocontrollable biomaterials.

Introduction

Light is a versatile, non-invasive and efficient stimulus with high spatial and temporal resolution and facile modulation. Photoswitches, of which azobenzenes are arguably the most common class, enable the control of functional materials with light.[1,2] The photoswitching of azobenzenes is based on their reversible *trans*(*E*)-to-*cis*(*Z*) isomerization. Depending on their structure, azobenzenes have varying *Z*-isomer thermal lifetimes and varying degrees of spectral separation between the absorption bands of the isomers. Conventional azobenzenes absorb ultraviolet or visible light with relatively high energy, which limits their applicability for emerging fields such as solar energy harvesting,[3] 3D printing,[4] photosensors,[5] photo-actuation[6] and photocatalysis.[7] When compared to longer wavelengths, UV excitation is hampered by, for example, its limited solar availability, non-specific absorption, and harm-fulness to organic materials and live cells.[8] Moreover, due to the

optical properties of biological tissue, photoswitching systems capable of operating under red or even near-infrared (NIR) light are of particular interest for biomedicine.[9–14]

Developing azobenzenes suitable for these aforementioned fields in terms of properties such as red-shifted excitation wavelengths, spectral resolution of *E*- and *Z*-isomers and thermal stability of the *Z*-isomer, requires structural modification;[15] a complex approach that generally involves extensive computational studies and synthesis. For example, *ortho*-functionalization of azobenzenes is an established approach to create photoswitches with a long *Z*-lifetime,[16,17] which is required for efficient photoswitching in both directions and precise control of the isomer composition. Despite recent advances, creating bistable red-absorbing azobenzenes remains a challenge, since red-shifting typically leads to drastically decreased thermal stability of the *Z*-isomer. Furthermore, there are no reports on bistable NIR-absorbing azobenzenes.[18,19]

Indirect excitation, *i.e.*, excitation that does not rely on the thermal relaxation or absorption bands of the *E*- and *Z*-isomers, but instead makes use of a proxy molecule to absorb light-activation signals, may overcome the foregoing issues of azobenzenes while retaining their beneficial intrinsic properties such as bistability and robustness. Intriguingly, indirect excitation allows tailoring and expansion of the photoswitching properties of the system without structural modification, even beyond the capabilities of the azobenzene itself. Isomerization by indirect excitation can be effected in various ways, such as photoinduced electron transfer,[20–22] two-photon absorption

[a]*Faculty of Engineering and Natural Sciences, Tampere University, FI-33101, Tampere, Finland. E-mail: arri.priimagi@tuni.fi; nikita.durandin@tuni.fi*

[b]*School of Chemical and Pharmaceutical Sciences, Technological University Dublin, City Campus, Kevin Street, Dublin 8, Ireland*

[c]*Institute of Microstructure Technology, Karlsruhe Institute of Technology, Hermann-von-Helmholtz-Platz 1, 76344 Eggenstein-Leopoldshofen, Germany*

[d]*Drug Research Program, Division of Pharmaceutical Biosciences, Faculty of Pharmacy, University of Helsinki, FI-00014, Helsinki, Finland*

† Electronic supplementary information (ESI) available. See DOI: 10.1039/d1sc01717a

induced energy transfer,[23] photon upconversion[24,25] and triplet sensitization.[26–30]

Triplet-sensitized Z-to-E isomerization of azobenzenes is an especially viable approach for indirect excitation due to its reversibility, non-destructivity and near-unity conversion efficiency.[26,29,31] Triplet sensitization has also been utilized to isomerize other types of photoswitches, such as overcrowded alkenes,[32] diarylethenes,[33] stilbenes[34] and indigos.[35] However, in previous reports triplet sensitizers have been excited in the UV-to-yellow (<580 nm) range, while the capabilities of potent red and NIR-absorbing triplet sensitizers, such as porphyrins, have not been utilized in azobenzene photoswitching. Thus, we set out to study this orthogonal excitation pathway for bistable azobenzenes and explore the wavelength limits of triplet-sensitized photoisomerization and how it improves the efficiency and control over photoswitching.

Here we demonstrate triplet-sensitized Z-to-E isomerization of azobenzenes under red and NIR excitation and establish its efficiency via kinetics studies. We have employed a NIR-absorbing porphyrin, PdNP (Pd(II)meso-tetraphenyltetranaphthoporhyrin[36–38]) and two commercially available red-absorbing porphyrins, PdP and PtP (Pd(II) and Pt(II)meso-tetraphenyltetrabenzoporphyrin, see Chart 1), as triplet photosensitizers. The sensitizers were used in combination with tetrafluoroazobenzene (TFA[39,40]) and fluoropyrrolidineazobenzene (FPA,[41] see Chart 1). Both ortho-functionalized azobenzenes exhibit efficient photoisomerization (>80% conversion to both Z- and E-isomers) under visible light and remarkably long thermal half-lives (days). TFA requires blue light (410 nm) for Z-to-E photoisomerization. In contrast, Z-FPA absorbs red light, albeit weakly, and thus it was used to compare photoisomerization under direct and triplet-sensitized excitation.

Results and discussion

Triplet energy transfer studies

All experiments were conducted in dimethyl sulfoxide (DMSO). Since triplet sensitizers generate reactive oxygen species under illumination, bis(methylthio)methane was added as an oxygen

scavenger.[42] To study the triplet energy transfer (TET) from PdP and PtP to the azobenzenes, we performed quenching studies by measuring the phosphorescence lifetimes of both sensitizers in the presence of E- or Z-isomers of both azobenzenes. The resulting Stern–Volmer plots of the quenching studies are shown in Fig. 1.

The Stern–Volmer rate constant (K_{SV}) yielded by the linear fit on the quenching data was then used to evaluate the rate constant of triplet energy transfer:

$$k_{TET} = \frac{K_{SV}}{\tau_0}, \tag{1}$$

where τ_0 is the unquenched phosphorescence lifetime of the sensitizer (260 μs and 46 μs for PdP and PtP, respectively). The quenching experiments are discussed in more detail in the ESI.† k_{TET} values were then used to calculate the triplet energy gap (ΔE_T) between the sensitizer and azobenzene triplet states:[43]

$$\frac{\Delta E_T}{k_B T} = \ln\left(\frac{k_{diff}}{k_{TET}} - 1\right), \tag{2}$$

where k_B is the Boltzmann constant, T is the temperature and k_{diff} ($= 1.1 \times 10^9$ M^{-1} s^{-1}) is the diffusion rate constant of the system (see the ESI†). Finally, the obtained ΔE_T values were used together with the sensitizer triplet energies (1.55 and 1.61 eV for PdP and PtP, respectively, see Fig. S3†) to evaluate the triplet energies (E_T) of both E- and Z-isomers of the azobenzenes. To our knowledge, these are the first reported triplet state energies of ortho-substituted azobenzenes. The k_{TET}, ΔE_T and E_T values of each pair are given in Table 1.

Interestingly, the Z-isomer of TFA has higher E_T than the E-isomer, which appears contrary to the unsubstituted azobenzene (E_T of Z-isomer 29 kcal mol^{-1} i.e. 1.29 eV), whereas the E_T values of E-TFA and E-FPA are comparable to the previously reported values for unsubstituted and para-substituted azobenzenes (33–35 kcal mol^{-1} i.e. 1.43–1.52 eV).[44,45] The kinetics studies results also reveal the
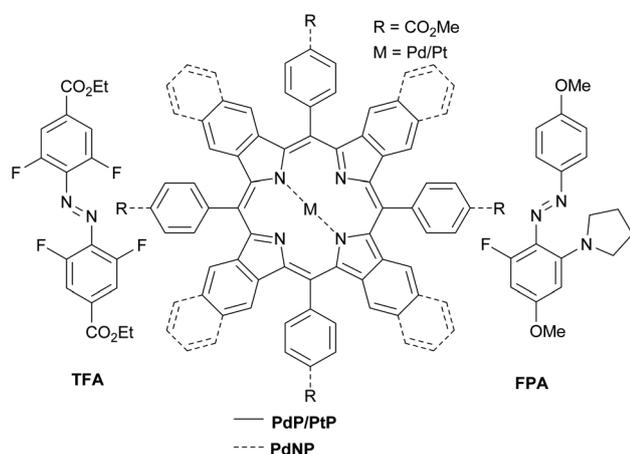

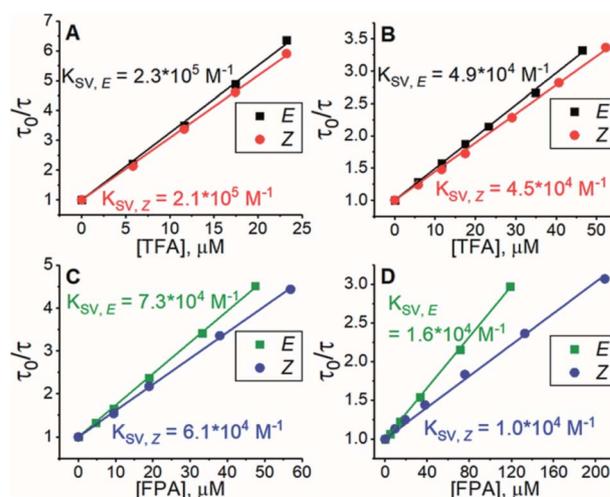Chart 1 Sensitizers and azobenzenes used in this study.

Fig. 1 Results of phosphorescence quenching. Stern–Volmer plots and the corresponding K_{SV} values of (A) TFA and PdP, (B) TFA and PtP, (C) FPA and PdP and (D) FPA and PtP.

Table 1 Rate constant of triplet energy transfer (k_{TET}), the triplet energy gap (ΔE_T) between the sensitizer and azobenzene, and the triplet energy (E_T) of the azobenzene derived from the quenching results

Pair	k_{TET} (M^{-1} s^{-1})	ΔE_T ($k_B T$)	ΔE_T (meV)	E_T (eV)
E-TFA/PdP	8.7×10^8	−1.3	−34	1.49–1.52
E-TFA/PtP	1.1×10^9	−4.7	−120	
Z-TFA/PdP	8.1×10^8	−1.0	−26	1.52–1.56
Z-TFA/PtP	9.7×10^8	−2.0	−52	
E-FPA/PdP	2.8×10^8	1.1	29	1.58–1.63
E-FPA/PtP	3.6×10^8	0.7	18	
Z-FPA/PdP	2.4×10^8	1.3	34	1.58–1.65
Z-FPA/PtP	2.2×10^8	1.4	36	

Fig. 2 The absorption spectra of the photoswitching systems consisting of PdP and PtP and TFA (A) and FPA (C) and their photo-isomerization curves (B) and (D). The concentration of the azobenzene was 150 μM and the concentration of the sensitizer was 1.2 mol% of the azobenzene, *i.e.* 1.8 μM. The colored sections indicate the wavelength and time ranges used for photoswitching. The excitation light is on during the times indicated by the representative colors. Gray lines in (A) and (C) indicate the wavelength used for monitoring the isomerization. The observed partial E-to-Z isomerization of the azobenzenes, especially in case of TFA due to its small molar extinction coefficient at 525 nm, is caused by the competitive absorption of the azobenzene and the sensitizer.
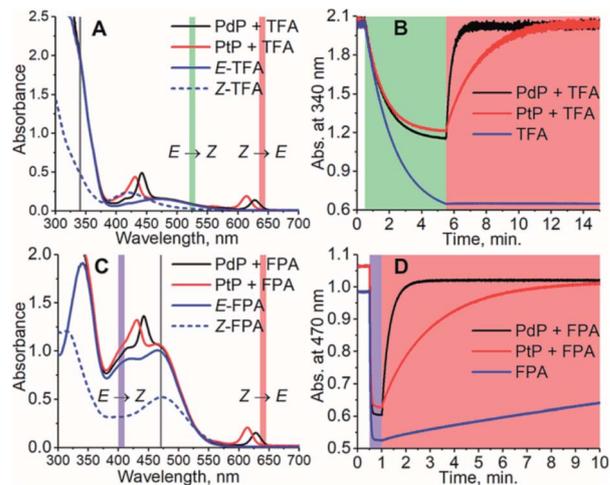
thermodynamics between the sensitizer and azobenzene: triplet energy transfer from both PdP and PtP appears exothermic for TFA (negative ΔE_T), while the lower values of k_{TET} between the sensitizers and FPA indicate endothermic energy transfer (positive ΔE_T).

Triplet-sensitized isomerization with red light

To study the effect of the triplet energies on photo-isomerization, we employed both PdP and PtP for photo-switching of TFA and FPA. In agreement with previous works,[26,28,29] E-to-Z isomerization was negligible on excitation of the sensitizer. This was observed although k_{TET} of the E-isomer is larger than for the Z-isomer for both TFA and FPA. However, after isomerizing the azobenzenes to their Z-configuration by direct excitation of the E-isomer (525 nm for TFA and 405 nm for FPA), rapid and nearly complete Z-to-E isomerization could be readily induced under 640 nm excitation using catalytic amounts (1.8 μM *i.e.* 1.2 mol% with respect to the azobenzene) of each sensitizer (see Fig. 2). An exponential function was fitted to the isomerization data to determine the rates of isomerization ($r_{Z \to E}$). The resulting fits are shown in Fig. S12–S16.† The rates of Z-to-E isomerization are clearly increased by several orders of magnitude by indirect excitation *via* the triplet energy transfer route. For example, the photoisomerization rate for FPA by triplet sensitization was over 100 times faster than that under 640 nm direct excitation (3.10 min^{-1} *versus* 0.028 min^{-1}). As expected, no isomerization of TFA without sensitizers was observed under 640 nm excitation. Notably, the sensitized photoswitching of FPA, for which TET is endothermic and thus slower, occurs as rapidly as photoswitching of TFA.

The conversion efficiency of sensitized Z-to-E isomerization ($\Phi_{Z \to E}$) was determined from the curves as the ratio of initial (dark) and final (achieved upon sensitization) absorbances. All values were close to unity, and only a minor difference in the conversion efficiency was observed between TFA and FPA. $r_{Z \to E}$ and $\Phi_{Z \to E}$ values of each sensitizer/azobenzene pair are shown in Table 2.

Surprisingly, the sensitizers appear to catalyze the Z-to-E isomerization of FPA even in the dark (see Fig. S18†). This increase in the rate of the thermal isomerization is especially pronounced with PtP as the contribution of the dark reaction to the overall observed rate is 31% (0.15 min^{-1}). In case of FPA/

Table 2 Rates ($r_{Z \to E}$) and efficiency ($\Phi_{Z \to E}$) of the photoisomerization under 640 nm excitation

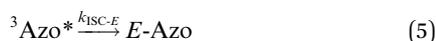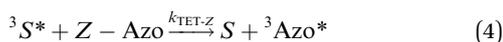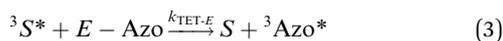| Pair	TFA/PdP	TFA/PtP	FPA/PdP	FPA/PtP
$r_{Z \to E}$ (min^{-1})	3.10	0.50^a	3.10	0.49^a
$\Phi_{Z \to E}$ (%)	99	99	96	96

^{a} The smaller $\Phi_{Z \to E}$ yielded by PtP results mainly from a smaller spectral overlap between the absorption and the excitation (see Fig. 2).

PdP, the contribution is only *ca.* 2% (0.06 min^{-1}). Also, the free base of the porphyrin (H$_2$P) catalyzes the isomerization of FPA in the dark (0.09 min^{-1}). This catalytic effect is perhaps a result of ground state coordination[46–48] between Z-FPA and the porphyrin. FPA has three π donors in *ortho*- and *para*-positions and only one electron-withdrawing fluorine substituent, increasing the affinity of the azo bridge to an electron-deficient site such as a metal cation. This effect is not observed with the drastically electron-poorer TFA, which supports this explanation.

Mechanism of triplet-sensitized isomerization

To better understand the observed results of triplet-sensitized photoswitching and the considerably increased isomerization rates, we conducted an analysis of the underlying reaction mechanisms that can be described with the following set of equations:[26,29]

$$^3S^* + E - \text{Azo} \xrightarrow{k_{\text{TET-}E}} S + {}^3\text{Azo}^* \qquad (3)$$

$$^3S^* + Z - \text{Azo} \xrightarrow{k_{\text{TET-}Z}} S + {}^3\text{Azo}^* \qquad (4)$$

$$^3\text{Azo}^* \xrightarrow{k_{\text{ISC-}E}} E\text{-Azo} \qquad (5)$$

$$^3\text{Azo}^* \xrightarrow{k_{\text{ISC-}Z}} Z\text{-Azo} \qquad (6)$$

where S is the sensitizer, superscript 3 is the triplet state, ISC is the intersystem crossing between the singlet and triplet states and k denotes the rate constant of each process. $k_{\text{TET-}E}$ and $k_{\text{TET-}Z}$ are determined experimentally and given in Table 1. It is also important to notice, that $^3\text{Azo}^*$ can be considered as a common state between the isomers, since there is no energy barrier associated with the CNNC twist in the triplet manifold.[49,50] While there are no direct observations reported on the triplet lifetime of azobenzenes, the commendable computational work[49] by Cembran *et al.* estimates $k_{\text{ISC-}E}$ as 10^{11} s^{-1}. The ultrafast ISC results from the degeneracy between the minimum of the triplet state and the intersection between the triplet state and ground state of *E*-Azo. Since the photostationary composition yielded by sensitized isomerization can be derived from the equations above as[26,29]

$$\frac{[E\text{-Azo}]}{[Z\text{-Azo}]} = \frac{k_{\text{TET-}Z}}{k_{\text{TET-}E}} \frac{k_{\text{ISC-}E}}{k_{\text{ISC-}Z}}, \qquad (7)$$

we can use $\Phi_{Z \to E}$ and the TET results to estimate relative $k_{\text{ISC-}Z}$ for TFA (10^9 s^{-1}) and FPA (3×10^9 s^{-1}), corresponding roughly to 1–3% of $k_{\text{ISC-}E}$. This also explains why triplet sensitization of azobenzenes leads almost exclusively to the formation of the *E*-isomer.[26,29,49]

Based on the isomerization kinetics, even endothermic TET (as is the case with FPA) is apparently capable of driving isomerization efficiently. This indicates that the whole process of triplet-sensitized isomerization is largely entropy-driven,[51,52] since the rate of the isomerization is fairly decoupled from the change in enthalpy involved in TET. The change in entropy (ΔS) of TET is[51]

$$\Delta S = k_{\text{B}} \ln \left(\frac{[Z - \text{Azo}] \, [^3S^*]}{[S] \, [^3\text{Azo}^*]} \right). \qquad (8)$$

The ultrafast crossing between the triplet state and the ground state of *E*-Azo (eqn (5)) leads to $[^3\text{Azo}^*] \ll [Z\text{-Azo}], [^3S^*], [S]$ and ensures a large entropy component in the triplet-sensitized isomerization. This also effectively eliminates the azobenzene-to-sensitizer reverse TET.[52] Therefore, even photosensitizers with considerably lower triplet energies are still capable of sensitizing the *Z*-to-*E* isomerization of azobenzenes, which enables the expansion of excitation wavelengths to the deeper red and even into NIR regions.

Triplet-sensitized isomerization with near-infrared light

Prompted by this finding, we combined TFA with PdNP, a sensitizer with a triplet energy of 1.30 eV and strong

absorption in the NIR region (see Fig. S2 and S4†). The triplet energy gap of this pair is thus ≥ 220 meV, *i.e.*, 8.5 $k_{\text{B}}T$, and as a result, TET is highly endothermic. Nonetheless, photoisomerization under 740 nm excitation was, to our delight, efficient despite this remarkably high endothermic energy gap (see Fig. 3). PdNP was capable of sensitizing isomerization of TFA even under 770 nm excitation ($r_{Z \to E} = 0.93$ min^{-1}, see Fig. S14†).

Thanks to the bistable nature and rapid triplet-sensitized isomerization of TFA under NIR excitation, the isomer composition can be precisely controlled by modulating the excitation dose (duration and/or intensity). This stepwise photoisomerization by dosed excitation is shown in Fig. 4. Repeatable cyclic switching between isomers is also typically desired for applications of photoswitching. This can be achieved in triplet-sensitized photoswitching systems by alternating excitation of the azobenzene and sensitizer as shown in Fig. 4 No discernible change in the rate of sensitized isomerization and only a slight
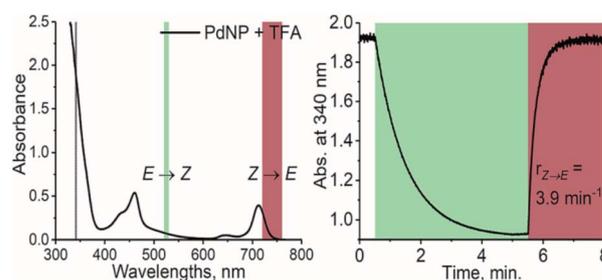

Fig. 3 Absorption spectrum of PdNP and TFA (left) and the photoisomerization curve (right) under 525 nm (green color) and 740 nm (dark red) excitation with the resulting rates of isomerization.
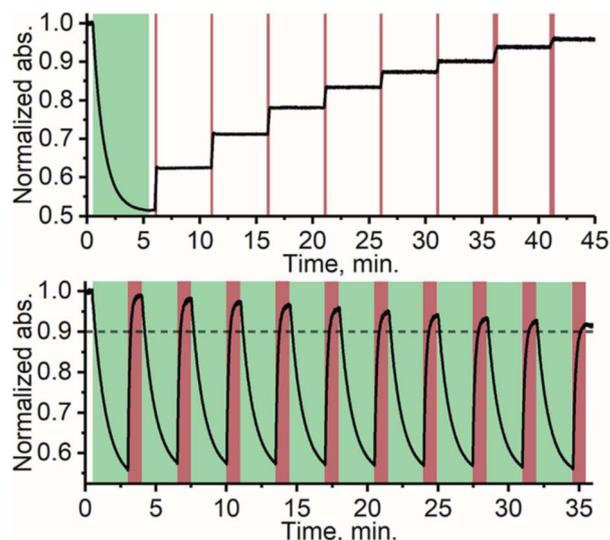

Fig. 4 Stepwise photoisomerization (above) of TFA by exciting PdNP with 10 s (last two were 20 s) doses of 740 nm excitation (dark red bars) in 5 min intervals. Cyclic photoswitching (below) of TFA/PdNP with 10 cycles of alternating 525 nm (direct excitation of *E*-TFA, green sections) and 740 nm (excitation of PdNP, dark red sections) excitation wavelengths.

decrease in efficiency (less than 10%, likely due to photo-bleaching) was observed in 10 cycles. Photoswitching is achievable even in the presence of oxygen (Fig. S19†), when the effects of singlet oxygen generated by the photosensitizer are mitigated by employing oxygen-scavengers.

Conclusions

We have shown that photoisomerization of bistable *ortho*-functionalized azobenzenes *via* triplet energy transfer is rapid with near-unity efficiency under red and near-infrared (up to 770 nm) excitation. Detailed studies of the kinetics indicate that triplet-sensitized isomerization is largely entropy-driven. Thus, even sensitizers with triplet energies considerably lower than those of the azobenzenes used are still capable of effectively sensitizing the isomerization. This was confirmed by using an azobenzene/sensitizer pair with an endothermic triplet energy gap of over 200 meV between them. The major entropy-factor involved in the process also projects that this excitation pathway is efficient for any azobenzene. This expands the properties of photoswitching systems without chemically modifying the photoswitch itself. Combined with the desirable use of red/NIR excitation, precise control of isomer composition, and repeatable cyclic isomerization, we envision that this approach will emerge as a potent tool for low-energy photoswitching in light-responsive materials.

Conflicts of interest

There are no conflicts to declare.

Acknowledgements

Notes and references

1 A. Goulet-Hanssens, F. Eisenreich and S. Hecht, *Adv. Mater.*, 2020, **32**, 1905966.

2 D. Dattler, G. Fuks, J. Heiser, E. Moulin, A. Perrot, X. Yao and N. Giuseppone, *Chem. Rev.*, 2020, **120**, 310–433.

3 L. Dong, Y. Feng, L. Wang and W. Feng, *Chem. Soc. Rev.*, 2018, **47**, 7339–7368.

4 D. Ahn, L. M. Stevens, K. Zhou and Z. A. Page, *ACS Cent. Sci.*, 2020, **6**, 1555–1563.

5 X. Zhou, T. Zifer, B. M. Wong, K. L. Krafcik, F. Léonard and A. L. Vance, *Nano Lett.*, 2009, **9**, 1028–1033.

6 J. Boelke and S. Hecht, *Adv. Opt. Mater.*, 2019, **7**, 1900404.

7 B. M. Neilson and C. W. Bielawski, *ACS Catal.*, 2013, **3**, 1874–1885.

8 M. Zayat, P. Garcia-Parejo and D. Levy, *Chem. Soc. Rev.*, 2007, **36**, 1270–1281.

9 M. Dong, A. Babalhavaeji, S. Samanta, A. A. Beharry and G. A. Woolley, *Acc. Chem. Res.*, 2015, **48**, 2662–2670.

10 M. J. Fuchter, *J. Med. Chem.*, 2020, **63**, 11436–11447.

11 D. Bléger and S. Hecht, *Angew. Chem., Int. Ed.*, 2015, **54**, 11338–11349.

12 S. Samanta, A. A. Beharry, O. Sadovski, T. M. McCormick, A. Babalhavaeji, V. Tropepe and G. A. Woolley, *J. Am. Chem. Soc.*, 2013, **135**, 9777–9784.

13 I. M. Welleman, M. W. H. Hoorens, B. L. Feringa, H. H. Boersma and W. Szymański, *Chem. Sci.*, 2020, **11**, 11672–11691.

14 K. Hüll, J. Morstein and D. Trauner, *Chem. Rev.*, 2018, **118**, 10710–10747.

15 H. M. D. Bandara and S. C. Burdette, *Chem. Soc. Rev.*, 2012, **41**, 1809–1825.

16 D. Bléger, J. Schwarz, A. M. Brouwer and S. Hecht, *J. Am. Chem. Soc.*, 2012, **134**, 20597–20600.

17 M. J. Hansen, M. M. Lerch, W. Szymanski and B. L. Feringa, *Angew. Chem., Int. Ed.*, 2016, **55**, 13514–13518.

18 M. Dong, A. Babalhavaeji, C. V Collins, K. Jarrah, O. Sadovski, Q. Dai and G. A. Woolley, *J. Am. Chem. Soc.*, 2017, **139**, 13483–13486.

19 D. B. Konrad, G. Savasci, L. Allmendinger, D. Trauner, C. Ochsenfeld and A. M. Ali, *J. Am. Chem. Soc.*, 2020, **142**, 6538–6547.

20 A. Goulet-Hanssens, M. Utecht, D. Mutruc, E. Titov, J. Schwarz, L. Grubert, D. Bléger, P. Saalfrank and S. Hecht, *J. Am. Chem. Soc.*, 2017, **139**, 335–341.

21 A. Goulet-Hanssens, C. Rietze, E. Titov, L. Abdullahu, L. Grubert, P. Saalfrank and S. Hecht, *Chem*, 2018, **4**, 1740–1755.

22 G. L. Hallett-Tapley, C. D'Alfonso, N. L. Pacioni, C. D. McTiernan, M. González-Béjar, O. Lanzalunga, E. I. Alarcon and J. C. Scaiano, *Chem. Commun.*, 2013, **49**, 10073–10075.

23 J. Moreno, M. Gerecke, L. Grubert, S. A. Kovalenko and S. Hecht, *Angew. Chem., Int. Ed.*, 2016, **55**, 1544–1547.

24 Z. Jiang, M. Xu, F. Li and Y. Yu, *J. Am. Chem. Soc.*, 2013, **135**, 16446–16453.

25 L. Wang, H. Dong, Y. Li, C. Xue, L.-D. Sun, C.-H. Yan and Q. Li, *J. Am. Chem. Soc.*, 2014, **136**, 4480–4483.

26 L. B. Jones and G. S. Hammond, *J. Am. Chem. Soc.*, 1965, **87**, 4219–4220.

27 J. Ronayette, R. Arnaud, P. Lebourgeois and J. Lemaire, *Can. J. Chem.*, 1974, **52**, 1848–1857.

28 J. Ronayette, R. Arnaud and J. Lemaire, *Can. J. Chem.*, 1974, **52**, 1858–1867.

29 P. Bortolus and S. Monti, *J. Phys. Chem.*, 1979, **83**, 648–652.

30 A. Goulet-Hanssens, C. Rietze, E. Titov, L. Abdullahu, L. Grubert, P. Saalfrank and S. Hecht, *Chem*, 2018, **4**, 1740–1755.

31 A. Cembran, F. Bernardi, M. Garavelli, L. Gagliardi and G. Orlandi, *J. Am. Chem. Soc.*, 2004, **126**, 3234–3243.

32 A. Cnossen, L. Hou, M. M. Pollard, P. V Wesenhagen, W. R. Browne and B. L. Feringa, *J. Am. Chem. Soc.*, 2012, **134**, 17613–17619.

33 S. Fredrich, T. Morack, M. Sliwa and S. Hecht, *Chem.–Eur. J.*, 2020, **26**, 7672–7677.

34 J. A. Mercer-Smith and D. G. Whitten, *J. Am. Chem. Soc.*, 1978, **100**, 2620–2625.

35 G. M. Wyman, B. M. Zarnegar and D. G. Whitten, *J. Phys. Chem.*, 1973, **77**, 2584–2586.

36 J. E. Rogers, K. A. Nguyen, D. C. Hufnagle, D. G. McLean, W. Su, K. M. Gossett, A. R. Burke, S. A. Vinogradov, R. Pachter and P. A. Fleitz, *J. Phys. Chem. A*, 2003, **107**, 11331–11339.

37 V. V Rozhkov, M. Khajehpour and S. A. Vinogradov, *Inorg. Chem.*, 2003, **42**, 4253–4255.

38 O. S. Finikova, S. E. Aleshchenkov, R. P. Briñas, A. V Cheprakov, P. J. Carroll and S. A. Vinogradov, *J. Org. Chem.*, 2005, **70**, 4617–4628.

39 D. Bléger, J. Schwarz, A. M. Brouwer and S. Hecht, *J. Am. Chem. Soc.*, 2012, **134**, 20597–20600.

40 C. Knie, M. Utecht, F. Zhao, H. Kulla, S. Kovalenko, A. M. Brouwer, P. Saalfrank, S. Hecht and D. Bléger, *Chem.–Eur. J.*, 2014, **20**, 16492–16501.

41 Z. Ahmed, A. Siiskonen, M. Virkki and A. Priimagi, *Chem. Commun.*, 2017, **53**, 12520–12523.

42 D. Dzebo, K. Moth-Poulsen and B. Albinsson, *Photochem. Photobiol. Sci.*, 2017, **16**, 1327–1334.

43 K. Sandros, *Acta Chem. Scand.*, 1964, **18**, 2355–2374.

44 S. Monti, E. Gardini, P. Bortolus and E. Amouyal, *Chem. Phys. Lett.*, 1981, **77**, 115–119.

45 S. Monti, S. Dellonte and P. Bortolus, *J. Photochem.*, 1983, **23**, 249–256.

46 A. Nakamura, K. Doi, K. Tatsumi and S. Otsuka, *J. Mol. Catal.*, 1976, **1**, 417–429.

47 S. Ciccone and J. Halpern, *Can. J. Chem.*, 1959, **37**, 1903–1910.

48 Z. Wang, R. Losantos, D. Sampedro, M. Morikawa, K. Börjesson, N. Kimizuka and K. Moth-Poulsen, *J. Mater. Chem. A*, 2019, **7**, 15042–15047.

49 A. Cembran, F. Bernardi, M. Garavelli, L. Gagliardi and G. Orlandi, *J. Am. Chem. Soc.*, 2004, **126**, 3234–3243.

50 L. Gagliardi, G. Orlandi, F. Bernardi, A. Cembran and M. Garavelli, *Theor. Chem. Acc.*, 2004, **111**, 363–372.

51 Y. Y. Cheng, B. Fückel, T. Khoury, R. G. C. R. Clady, N. J. Ekins-Daukes, M. J. Crossley and T. W. Schmidt, *J. Phys. Chem. A*, 2011, **115**, 1047–1053.

52 J. Isokuortti, S. R. Allu, A. Efimov, E. Vuorimaa-Laukkanen, N. V. Tkachenko, S. A. Vinogradov, T. Laaksonen and N. A. Durandin, *J. Phys. Chem. Lett.*, 2020, **11**, 318–324.